Andreev scattering and the Kondo effect

Aashish A. Clerk and Vinay Ambegaokar
Laboratory of Atomic and Solid State Physics, Cornell University, Ithaca, New York 14853

Selman Hershfield
Department of Physics, University of Florida, Gainesville, Florida 32611
(Received 21 July 1999)

The properties of an infinite-U Anderson impurity coupled to both normal and superconducting metals is studied using a generalization of the noncrossing approximation which incorporates multiple Andreev reflection. Both the cases of a quantum dot and a point contact containing an impurity are considered. We find that the magnitude of the Kondo resonance is altered, and that structure develops at energies corresponding to the superconducting gap. This leads to observable changes in the zero-bias conductance. We also find that magnetic and nonmagnetic Kondo effects respond in opposite manners to Andreev reflection.

I. INTRODUCTION

Though the Kondo effect is far from being a new problem in condensed matter physics, the question of what occurs when one places a Kondo impurity on the normal side of a normal-superconducting (NS) interface has only recently received attention.[1–4] The NS case is significantly different from the more studied problem of a magnetic impurity in a bulk superconductor, in which a lack of low-lying excitations leads to a suppression of the Kondo effect. In the present problem, we have both the existence of low lying excitations (provided by the normal metal) and anomalous pair correlations (a result of the proximity effect). The question of what influence this combination will have on the dynamically generated Kondo effect is the subject of this work. In particular, how will the sharp Kondo resonance at the Fermi energy be modified?

It should be noted that the immediate motivation for studying this problem has come from experiment. Recent results obtained from semiconductor quantum dots have shown clear signs of the Kondo effect,[5,6] leading to the question of what one would expect if a quantum dot were now coupled to both normal and superconducting leads. In another class of systems, zero-bias conductance anomalies seen in metallic point contacts have been attributed to scattering off effective nonmagnetic, two channel Kondo impurities.[7,8] Such point contacts can be constructed between normal and superconducting metals,[9] providing further relevance for the current problem.

II. THE MODELS

In this work, we study three different systems: a quantum dot coupled to both normal and superconducting leads (NS-QDOT), a point contact between normal and superconducting metals which contains a magnetic impurity (M-QPC), and a normal-superconducting point contact which contains a nonmagnetic, two-channel Kondo impurity (NM-QPC). We outline in this section the models used for each of these devices.

For the first system, the NS-QDOT, we treat the quantum dot as an infinite-U Anderson impurity coupled to both normal and superconducting leads. The infinite-U Anderson model has been used successfully in the absence of superconductivity to describe the Kondo effect in quantum dots; our model represents a natural generalization to the NS case. Using a slave-boson representation, we have

$$H_{\rm dot}=H_0+\varepsilon_d\sum_\sigma f_\sigma^\dagger f_\sigma+W\sum_{\alpha,k,\sigma}(c_{\alpha,k\sigma}^\dagger b^\dagger f_\sigma+\text{H.c.}), \quad (1)$$

$$H_0=\sum_{\alpha,k,\sigma}\varepsilon_k c_{\alpha,k\sigma}^\dagger c_{\alpha,k\sigma}+\sum_k(\Delta c_{S,k\uparrow}^\dagger c_{S,-k\downarrow}^\dagger+\text{H.c.}). \quad (2)$$

The $c_{\alpha,k\sigma}^\dagger$ operators here create band electrons, with σ denoting spin and $\alpha=N,S$ labeling the two leads. Δ represents the pair potential in the superconducting lead. The Anderson impurity has bare energy ε_d, and is represented in the usual manner using auxiliary fermion (f) and boson (b) operators; the $U=\infty$ constraint of single occupancy takes the form $\Sigma_\sigma f_\sigma^\dagger f_\sigma+b^\dagger b=1$.

For the NS point contact with magnetic impurity system (M-QPC), we use a model consisting of a rectangular wire of transverse dimensions w, extended in the z direction and having a step-function pair potential $\Delta(z)=\Theta(z)\Delta$. The magnetic impurity is modeled as an infinite-U Anderson impurity sitting at a point a on the NS interface:

$$H_m=H_{Q0}+\varepsilon_d\sum_\sigma f_\sigma^\dagger f_\sigma+W\sum_\sigma[\Psi_\sigma^\dagger(\mathbf{a})b^\dagger f_\sigma+\text{H.c.}], \quad (3)$$

where $\Psi_\sigma^\dagger(\mathbf{x})$ creates a band electron at position $\mathbf{x}$ and

$$H_{Q0}=\int d\mathbf{x}\left[\sum_\sigma\Psi_\sigma^\dagger(\mathbf{x})\left(\frac{-\hbar^2\nabla^2}{2m}-E_F\right)\Psi_\sigma(\mathbf{x})+\Delta(z)\Psi_\uparrow^\dagger(\mathbf{x})\Psi_\downarrow^\dagger(\mathbf{x})+\text{H.c.}\right]. \quad (4)$$

For the final system of an NS point contact containing a nonmagnetic, two-channel impurity (NM-QPC), we use a

model similar to that for the M-QPC system. Now, however, the impurity represents a two-level system (TLS) off which electrons may scatter causing level-flips of the TLS.[10] In this model, the impurity does not carry ordinary spin, but rather has a pseudospin index τ which can take on one of two values, corresponding to the two states of the TLS. The interaction here between impurity and conduction electrons is also nonmagnetic, meaning that electron spin must be conserved. This is accomplished by having the slave-bosons carry a spin index. We have

$$H_{nm}=H_{Q0}+\varepsilon_d\sum_{\sigma} f_{\sigma}^{\dagger}f_{\sigma}+W\sum_{\sigma,\tau}[\Psi_{\sigma,\tau}^{\dagger}(\mathbf{a})b_{\sigma}^{\dagger}f_{\tau}+\text{H.c.}], \tag{5}$$

where the conduction electron Hamiltonian H_{Q0} is as in Eq. (4), with the modification that the conduction electron operators also carry the pseudospin index τ. We take the pairing in Eq. (4) to be diagonal in this index, which is compatible with the usual interpretation of the pseudospin as a parity index.

It is important to note that there are significant differences between the three systems we study, as can be seen from their respective Hamiltonians. In the NS-DOT system, the N and S leads are *only* in contact through the impurity; all transport through the system will involve it. In the point contact systems, we have the opposite situation—the N and the S metals are in perfect contact, with the impurity acting only as an additional source of scattering at the interface.

The difference between the two point contact systems is also worth emphasizing. In the M-QPC system, our impurity is magnetic and thus conduction electron spin is not conserved—real spin flips can occur. In the NM-QPC system, conduction electron spin *is* conserved; only the auxiliary pseudospin index τ can undergo spin flips. This difference will prove to be crucial, due to the sensitivity to spin ordering of the singlet pairing in the superconductor.

III. EXTENSION OF THE NONCROSSING APPROXIMATION

For all three of our systems, we calculate the impurity spectral function (also called the impurity density of states) using an extension of the self-consistent noncrossing approximation (NCA).[11] The NCA amounts to an infinite resummation of perturbation theory, and has been shown to be quantitatively reliable down to temperatures well below T_K.[11] We modify the NCA to now include multiple-Andreev reflection processes. The resulting NS-NCA f fermion and slave boson propagators are given in Fig. 1. The new graphs in our approximation are those which contain anomalous propagators; they do not appear in the usual NCA.

Like the original NCA, the NS-NCA is a conserving approximation as it may be derived by differentiating a generating functional (i.e., it is Φ derivable).[13] Moreover, if N is the degeneracy of the Anderson impurity, the NS-NCA includes *all* graphs to order $1/N$, including new Andreev reflection graphs which first appear at this order. As the success of the normal NCA is attributed to the fact that it too is exact to order $1/N$ (in the absence of superconductivity), the NS-NCA employed here can be viewed as a natural extension to NS Kondo systems.[12]

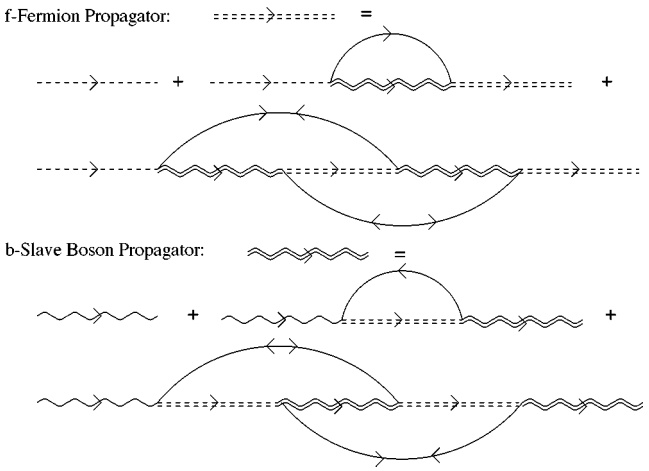

FIG. 1. Diagrammatic representation of the NS-NCA. Dashed lines are f fermions, wavy lines are slave bosons, solid lines are lead electrons. Double lines indicate a fully dressed propagator. Anomalous propagators indicate Andreev reflection.

It should be noted that previous studies of NS Kondo systems have either completely neglected changes in impurity dynamics due to superconductivity,[1] or have relied on the equations of motion approach which is formally only valid at temperatures above the Kondo temperature.[2] In analogy to the usual NCA, we expect our approach based on the NS-NCA to be quantitatively valid for temperatures well below T_K.

The Dyson equations pictured diagrammatically in Fig. 1 lead to a set of coupled integral equations for the f fermion and slave boson propagators. Letting $F(\omega)=[\omega-\varepsilon_d-\Sigma(\omega)]^{-1}$ and $B(\omega)=[\omega-\Pi(\omega)]^{-1}$ represent the f fermion and slave boson retarded propagators respectively, the equations read

$$\Sigma(\omega)=\frac{M\Gamma}{\pi}\int d\varepsilon\Big(\rho(\epsilon)B(\omega-\varepsilon)f(-\varepsilon) \mp\frac{\Gamma}{\pi}\int d\varepsilon'\alpha(\varepsilon)\alpha(\varepsilon')B(\omega+\varepsilon)F(w+\varepsilon+\varepsilon') \times B(\omega+\varepsilon')\Big), \tag{6}$$

$$\Pi(\omega)=\frac{2\Gamma}{\pi}\int d\varepsilon\Big(\rho(\epsilon)F(\omega+\varepsilon)f(\varepsilon) \pm\frac{\Gamma}{\pi}\int d\varepsilon'\alpha(\varepsilon)\alpha(\varepsilon')F(\omega+\varepsilon)B(w+\varepsilon+\varepsilon') \times F(\omega+\varepsilon')\Big). \tag{7}$$

In these equations, M is the channel degeneracy of the impurity—it equals 1 for both the NS-$QDOT$ and the M-QPC systems, and equals two for the NM-QPC system (where the two conserved values of electronic spin play the role of the two channels). The upper (lower) sign corresponds to the $M=1$ ($M=2$) systems. $\rho(\varepsilon)$ is the electronic density of states, $\Gamma=\pi W^2\rho(0)$ the bare tunneling rate, f the

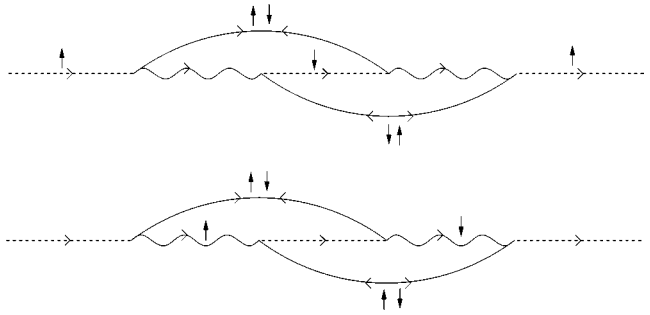

FIG. 2. Diagrammatic argument for the different sign of the Andreev reflection graphs in Eqs. (6). The first line shows a typical double Andreev reflection event for a magnetic impurity. The impurity carries a spin index in this case (i.e., the dashed propagator), and we see that both Andreev reflections are related by time reversal symmetry. The second line shows the situation for a nonmagnetic impurity. Here, the impurity itself does not carry a spin, but the slave-boson (wavy line) does in order to conserve spin. The two Andreev reflections in this case are *not* time reversed partners; the second is off by a spin rotation.

Fermi distribution function, and $\alpha(\varepsilon)$ is an effective electron-hole coherence parameter defined by

$$\alpha(\omega)=\sum_n u_n^*(\mathbf{a})v_n(\mathbf{a})\delta(|\omega|-\varepsilon_n)f(\omega), \tag{8}$$

where u_n and v_n are the usual BCS coherence factors.

It is worth commenting at this point on why the new Andreev reflection terms in Eqs. (6) and (7) enter with a different sign for the NM-QPC system compared to the *NS*-QDOT and *M*-QPC systems. The crucial difference has nothing to do with the channel symmetry of the impurity (i.e., 2 versus 1), but rather lies in the fact that the impurity-band interaction in the NM-QPC is nonmagnetic, whereas it is magnetic in the *NS*-QDOT and *M*-QPC systems. The fact that conduction electron spin must be conserved in the nonmagnetic case has a direct consequence on the sign of the double Andreev-reflection graph appearing in the *f*-fermion self-energy–the two Andreev reflections are not time-reversed partners, but are in fact off by a single spin rotation, leading to the additional factor of (-1) (recall that the BCS anomalous propagator changes sign under a spin rotation). This argument is displayed graphically in Fig. 2. A similar argument can be made to explain the sign difference occurring in the slave-boson graph.

We thus see that the new Andreev reflection processes which contribute to the dynamics of the impurity are sensitive to whether or not the impurity is magnetic; this is a direct consequence of the spin-sensitivity of the singlet pairing in the superconductor. This difference will have a significant consequence on how the Kondo effect is modified, as will be discussed in what follows.

IV. RESULTS

In all three of the systems considered, we choose model parameters corresponding to having the Anderson impurity in the Kondo regime, and use a Gaussian with halfwidth D for the normal-state density of states. Our choices of $\varepsilon_d=-0.67D$, $\Gamma=0.15D$ yield $T_K=0.0005D$ for a one-channel impurity (i.e., the *NS*-QDOT and *M*-QPC systems), and $T_K=0.0001D$ for a two-channel impurity (i.e., the NM-QPC system). We have numerically solved the *NS*-NCA equations in equilibrium for various temperatures and values of the superconducting gap. Within the NCA, the impurity spectral function $A_d(\omega)$ can be directly related to the *f*-fermion and slave boson spectral functions:

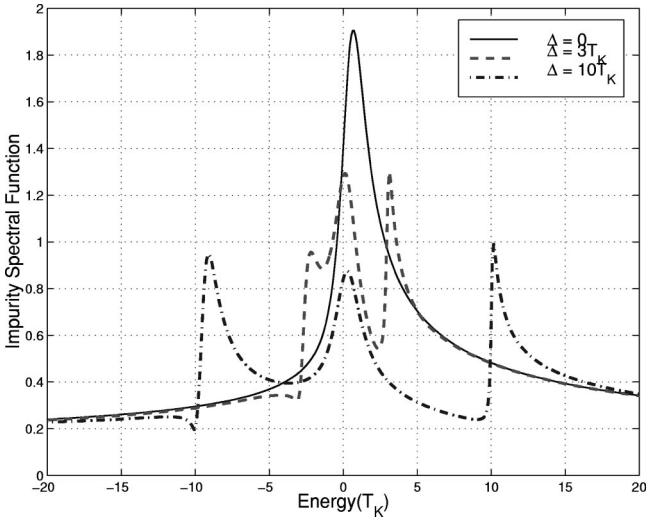

FIG. 3. NS QDOT spectral function $A_{d\sigma}(\omega)$ for various values of Δ at $T=0.5T_K$.

$$A_{d\sigma}(\omega)=\int d\varepsilon[e^{-\beta\varepsilon}+e^{-\beta(\varepsilon-\omega)}]A_{f\sigma}(\varepsilon)A_b(\varepsilon-\omega), \tag{9}$$

where the auxiliary particle spectral functions are defined by $A_f=-(1/\pi)\mathrm{Im}F$, $A_b=-(1/\pi)\mathrm{Im}B$. Note that the equality in Eq. (9) reflects a neglect of vertex corrections which is consistent with the large-N nature of the NCA.

A. NS quantum dot

In Fig. 3, we plot calculated spectral functions for the NS-QDOT system for several values of the superconducting gap Δ. In the case of no superconductivity ($\Delta=0$), we see as expected the emergence of the sharp Kondo resonance at the Fermi energy. As the superconductivity is gradually turned on, several interesting modifications of this resonance are observed.

The Kondo resonance does not vanish completely as Δ increases, though the spectral weight associated with the resonance clearly decreases, indicating a partial suppression of the Kondo effect. This is to be expected when one recalls that the ground state of a magnetic, one-channel Kondo impurity is one in which the local impurity screens its spin with low-energy conduction electrons. Turning on the superconductivity leads to a gap in the superconducting lead, and thus there are fewer low energy excitations available to the impurity to use in screening. It thus becomes more difficult to form the spin-screened Kondo ground state, resulting in a diminishing of the Kondo effect. A similar result for the NS QDOT is found using slave-boson mean-field theory,[4] where the effective Kondo temperature is found to fall as Δ is increased above T_K.

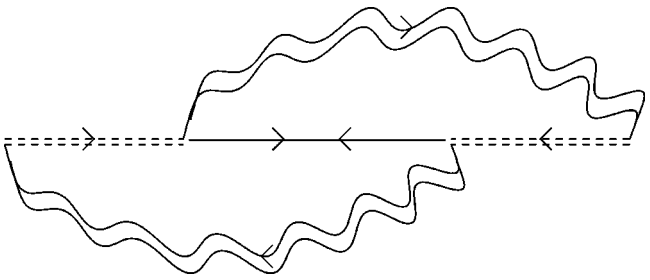

FIG. 4. Diagram used to calculate anomalous impurity propagator within the NCA. Double-dashed lines represent fully dressed f fermion, double wavy lines represent dressed slave boson propagators; both are calculated within the NS-NCA. The solid line represents an anomalous lead electron propagator.

Also of interest are the subpeaks which develop in the impurity spectral function at roughly $\pm\Delta$. These peaks are a result of the Kondo effect, and do not appear at higher temperatures. Recalling that the impurity spectral function at 0 temperature can be viewed as a local particle addition or removal spectrum, these peaks indicate that one can create a superconductinglike excited state with excitation energy Δ by adding a particle to the quantum dot. This indicates that *correlations are developing between the superconductor and the impurity*, implying that the superconducting electrons do indeed participate in the Kondo effect, even for $\Delta \gg T_K$. This can be substantiated by using the large-N variational approach[14] to calculate the approximate ground state of the NS-QDOT. One finds that there are superconducting quasiparticles present in the interacting ground state, with a weight that scales as T_K/Δ for large Δ.

As we find that a Kondo resonance persists in the NS-QDOT system, a natural question to ask is whether there is any resulting enhancement of the zero-bias conductance of the device, as is seen in the absence of superconductivity. The equilibrium spectral functions obtained for the NS-QDOT can be used to calculate the zero-bias Andreev conductance of the device, using an approximate formula derived in Ref. 2:

$$G_{NS}=\frac{4e^2}{h}\Gamma\int d\omega\,\mathrm{Re}\,\Sigma_{12}^{R}\mathrm{Im}(D_{12}^{R}D_{11}^{A})\left[-\frac{df}{d\omega}\right]. \quad (10)$$

Here, $D_{ij}^{R(A)}$ labels a component of the retarded (advanced) impurity Green function in Nambu-space, and $\Sigma_{ij}^{R(A)}$ is the corresponding self-energy. We have computed Eq. (10) within the NS-NCA, evaluating the anomalous impurity Green function from the diagram in Fig. 4 without use of the standard ''elastic'' approximation.[19]

For $T_K<\Delta<\Gamma$ and temperatures as low as one-half T_K, we find that the NS-QDOT *does not* exhibit a Kondo-induced enhancement of the zero-bias conductance, despite the presence of a Kondo resonance. This can be understood by the fact that in the infinite U limit, there is a suppression of pairing at the dot compared to the $U=0$ case. For energies and voltages smaller than Δ, the only processes to contribute to the current of the NS-QDOT are those in which two particles tunnel coherently through the dot and enter the superconductor as a pair. The suppression of pairing at the dot thus suppresses the zero bias conductance, despite the fact that there still is a Kondo resonance in the impurity spectral function. Note that the same conclusion is obtained using a correct equations-of-motion approach (see the erratum in Ref. 2).

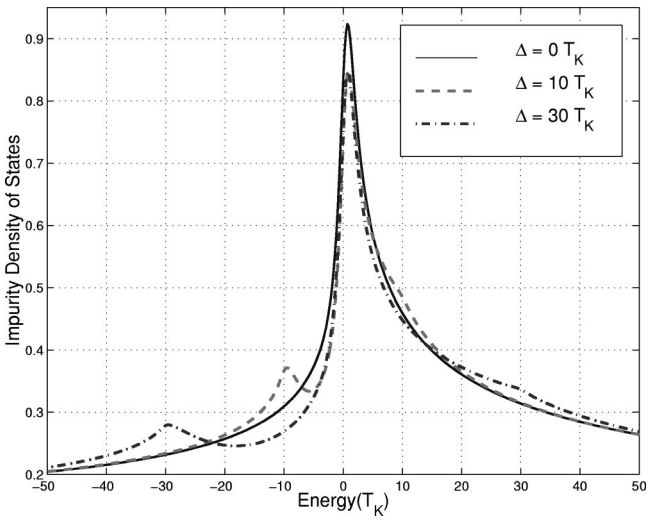

FIG. 5. Impurity spectral function $A_{d\sigma}(\omega)$ for a nonmagnetic two channel Anderson impurity in an NS-QPC for various values of Δ at $T=0.66T_K$. Note that the introduction of superconductivity reduces the height of the Kondo resonance.

B. NS point contact systems

We proceed to discuss results for the NS point contact with magnetic impurity (M-QPC) and NS point contact with nonmagnetic impurity (NM-QPC) systems. Shown in Fig. 5 is a plot of the impurity spectral function for the NM-QPC system for various values of Δ and at a temperature below the bare Kondo temperature; Fig. 6 shows a similar plot for the M-QPC system.

Several features are noteworthy in these plots. First, we notice that in both systems the introduction of superconductivity does not cause a significant change in the amount of spectral weight in the Kondo resonance. This indicates that

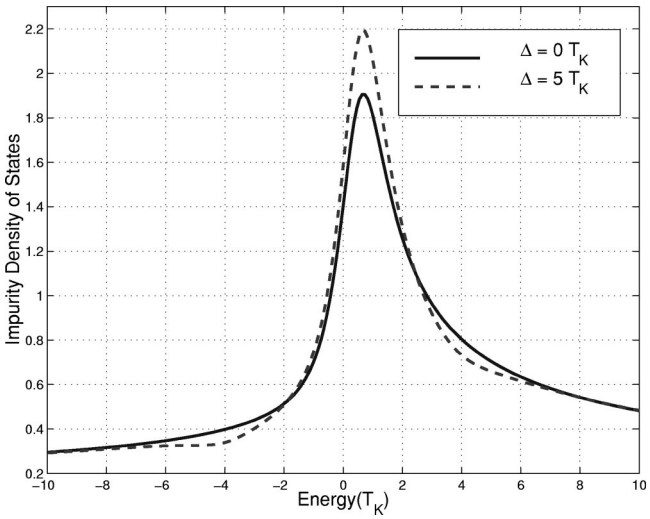

FIG. 6. Impurity spectral function $A_{d\sigma}(\omega)$ for a magnetic one channel Anderson impurity in an NS-QPC at $T=0.50T_K$. Note here that the introduction of superconductivity increases the height of the Kondo resonance.

there is no major suppression of the Kondo effect here, in contrast to the behavior observed in the *NS*-QDOT. This is to be expected—for a clean, ballistic *NS* point contact, an energy gap does not form at the position of the impurity (which is at the interface),[15] and consequently there is no shortage of the low energy excitations needed to generate the Kondo effect. This differs from the *NS*-QDOT, where the impurity is coupled directly to a bulk superconductor having a fully formed gap.

More interestingly, we find that in both point contact systems there is a small modification of the height of the Kondo peak when Δ is increased from 0. In the *NM*-QPC, we find that the Kondo peak is *reduced*, whereas the opposite is observed in the *M*-QPC—here, the Kondo peak is slightly *enhanced.*

This behavior can be understood heuristically as follows. First, note that by introducing superconductivity into the system, we introduce new processes which further couple the impurity to the conduction electrons (i.e., the multiple Andreev reflection processes which correspond to the new graphs included in the *NS*-NCA). These additional processes modify the effective coupling Γ between the impurity and conduction electrons; an increase of this coupling will enhance the Kondo effect, while a reduction will suppress it.[16] In the present case, the sign of this modification depends on whether or not the impurity is magnetic—as discussed in Sec. III, the new Andreev-reflection graphs enter with opposite signs in these two cases due to the sensitivity of Cooper pairing to spin ordering. This leads directly to the opposite behavior of the Kondo peak in the two cases.

The equilibrium impurity spectral functions can be used to derive the zero bias conductance for the point contact systems. We compute the current using the nonequilibrium Keldysh technique as was done in Refs. 17,18, restricting ourselves to the regime where $V,T \ll \Delta$. Using particle-hole symmetry, the zero bias conductance takes the form

$$G_{NS} = 2G_N - \frac{4e^2}{h}\pi\Gamma \int d\omega\, A_d(\omega)\left[-\frac{df}{d\omega}(\omega)\right], \quad (11)$$

where G_N is the normal-state Sharvin conductance of the point contact in the absence of the impurity. Details of this calculation are presented in the appendix. Note that we have neglected a term involving the anomalous impurity spectral function which is 0 for $T=0$ and is in general much smaller than the $A_d(\omega)$ term due to the strong suppression of on-site pairing.

The first term in Eq. (11) expresses the usual doubling of the conductance expected for an ideal *NS* point contact, while the second term represents the correction due to the impurity (δG_{NS}). As in the *N* case, the formation of the Kondo resonance will lead to a small suppression of the point contact conductance around zero voltage. The correction term due to the impurity in the absence of superconductivity (δG_N) has the same form as the second term in Eq. (11), but with an additional factor of 1/2.[18] If Andreev reflection did not effect the dynamics of the impurity, $A_d(\omega)$ would be identical in both the *NS* and *N* cases. We would thus expect the magnitude of the *NS* conductance anomaly to be *twice* that of the N anomaly.

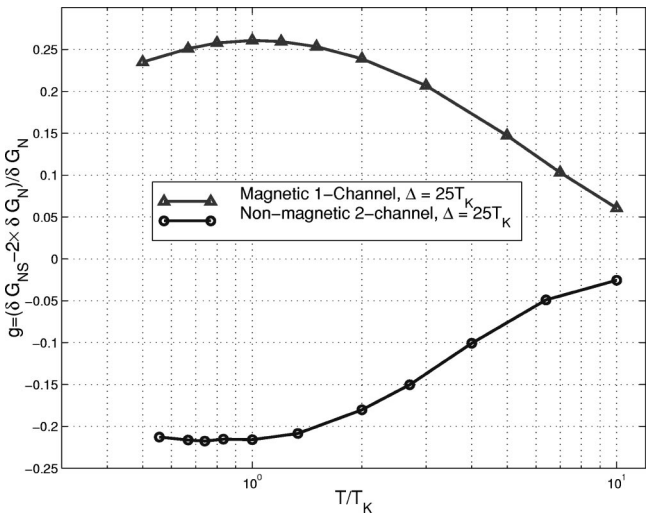

FIG. 7. Parameter $g=(\delta G_{\rm NS}-2\,\delta G_N)/\delta G_N$ for the *NS*-QPC as a function of temperature. The nonzero value of g is a consequence of changes in impurity dynamics due to Andreev reflection.

In Fig. 7, we plot the parameter $g=(\delta G_{NS}-2\delta G_N)/\delta G_N$ as a measure of the size of the *NS*-QPC zero bias anomaly. We see that as T is lowered below T_K, g becomes nonzero in both the cases of a magnetic and a nonmagnetic impurity, indicating that Andreev reflection does indeed have an observable impact on the Kondo effect in these systems. Note also that the sign of g in both cases is in accord with our discussion of the respective impurity spectral functions—in the magnetic case, the *NS* zero bias anomaly is *more* than two times the size of the anomaly in the normal state, while in the nonmagnetic case, the *NS* anomaly is *smaller* than twice the normal state anomaly. Again, magnetic and nonmagnetic Kondo effects respond in opposite ways to Andreev reflection. Significant too is the fact that the effect is large enough ($\pm 20\%$ at the lowest temperatures tested) that it should be experimentally accessible. This behavior could provide another test of the two-channel Kondo explanation of zero bias conductance anomalies seen in metallic point contacts.

V. CONCLUSION

We have studied the properties of three *NS* Kondo systems using an extension of the NCA which incorporates Andreev reflection. We find the Kondo effect is indeed modified by superconductivity in each system, leading to changes both in the impurity spectral function and in the zero-bias conductance. In the case of the *NS*-QDOT, superconductivity causes an overall decrease in the spectral weight of the Kondo resonance, and leads to the formation of new Kondo subpeaks at roughly $\pm\Delta$. There is no resulting enhancement of the zero-bias Andreev conductance due to the suppression of on-site pair correlations in the large-U limit. In the point contact with impurity systems, we find that superconductivity enhances the Kondo peak height in the case of a magnetic impurity, and suppresses it in the case of a nonmagnetic impurity. We attribute this difference to the sensitivity of Cooper pairing to spin ordering.

ACKNOWLEDGMENTS

This work was supported in part by the NSF under Grant No. DMR-9805613, and A.C. gratefully acknowledges financial support from the Olin Foundation. A.C. and V.A. also thank the Ørsted Laboratory of the Niels Bohr Institute and NORDITA for their hospitality.

APPENDIX: CONDUCTANCE OF AN NS POINT CONTACT WITH IMPURITY

We derive in this appendix Eq. (11) for the conductance of a constriction between a normal metal and a superconductor which contains an interacting impurity. Our technique is similar to that used in Ref. 18 to calculate the current of a normal metal point contact with an impurity. Here, however, the ''trick'' of combining currents calculated to the left and right of the constriction to eliminate the impurity lesser function cannot be used—we do not wish to deal with the complexities of calculating the supercurrent on the S side of our constriction. We instead focus solely on the current in the normal region, and use an approximate electron-hole symmetry which is present at low energies to eliminate the impurity lesser function.

We begin by writing the current in terms of the lesser Green function

$$I=-2ie\hbar\int\frac{d\omega}{2\pi}\int d^2x_\perp\left(\frac{\partial_z-\partial_{z'}}{2mi}\right)G^<(\mathbf{x},\mathbf{x}';\omega)|_{\mathbf{x}=\mathbf{x}'}, \tag{A1}$$

where $G^<(\mathbf{x},\mathbf{x}';\omega)$ is the Fourier transform in time of

$$G^<(\mathbf{x},t;\mathbf{x}',0)=i\langle\Psi_\uparrow^\dagger(\mathbf{x}',0)\Psi_\uparrow(\mathbf{x},t)\rangle. \tag{A2}$$

Note that we use only the 11 component of the matrix Nambu-Green function in computing the current; a factor of 2 is included in Eq. (A1) to account for spin. Note also that in what follows we neglect the pseudospin index τ which appears in the case of a two-channel Kondo impurity; our discussion may nevertheless be applied to this case by simply averaging over this index.

The next step in the derivation is to express the current in terms of the quasiparticle operators $\gamma_{n\sigma},\gamma_{n\sigma}^\dagger$ which appear when one makes a Bogolubov–de Gennes (B–dG) transformation to diagonalize the nonimpurity parts of the Hamiltonian [i.e., $\Psi_\uparrow(\mathbf{x})=\Sigma_n u_n(\mathbf{x})\gamma_{n\uparrow}-v_n^*(\mathbf{x})\gamma_{n\downarrow}^\dagger$, etc.]. This leads to the following identification:

$$G^<(\mathbf{x},\mathbf{x}';\omega)=[\hat\phi_{1,m}(\mathbf{x})]_i[\hat G_{mn}^<(\omega)]_{ij}[\hat\phi_{1,n}^*(\mathbf{x}')]_j \tag{A3}$$

with

$$\hat\phi_{1,m}(\mathbf{x})=\begin{pmatrix}u_m(\mathbf{x})\\-v_m^*(\mathbf{x})\end{pmatrix}, \tag{A4}$$

$$\hat\phi_{2,m}(\mathbf{x})=\begin{pmatrix}v_m(\mathbf{x})\\u_m^*(\mathbf{x})\end{pmatrix}, \tag{A5}$$

$$\hat G_{mn}^<(t)=i\begin{pmatrix}\langle\gamma_{n,\uparrow}^\dagger(0)\gamma_{m,\uparrow}(t)\rangle & \langle\gamma_{n,\downarrow}(0)\gamma_{m,\uparrow}(t)\rangle\\ \langle\gamma_{n,\uparrow}^\dagger(0)\gamma_{m,\downarrow}^\dagger(t)\rangle & \langle\gamma_{n,\downarrow}^\dagger(0)\gamma_{m,\downarrow}(t)\rangle\end{pmatrix}. \tag{A6}$$

In Eq. (A3), i and j are indices in particle-hole space, whereas m and n label different quasiparticle modes; we use the caret symbol to denote structure in particle-hole space. All repeated indices are to be summed over. Note that the B–dG wave functions u and v have a particularly simple form for mode energies ϵ less than the gap Δ.[20] Letting $\bar m$ index the transverse wave functions $\psi_{\bar m}(\mathbf{x}_\perp)$, we have for incident-electron modes

$$\hat\phi_{1,m}=\hat\phi_{1,(\bar m,\epsilon)}=\begin{pmatrix}\exp[ik_e(\epsilon)z]\\ \alpha(\epsilon)\exp[ik_h(\epsilon)z]\end{pmatrix}\psi_{\bar m}(\mathbf{x}_\perp), \tag{A7}$$

where $k_e=\sqrt{(2m/\hbar^2)(E_F+\epsilon-E_{\bar m})}$, $k_h=\sqrt{(2m/\hbar^2)(E_F-\epsilon-E_{\bar m})}$, and $\alpha=\exp[-i\arccos(\epsilon/\Delta)]$ is the Andreev reflection phase. E_F denotes the Fermi energy, while $E_{\bar m}$ is the energy of the transverse mode $\bar m$. Incident-hole wave functions have a similar form:

$$\hat\phi_{1,m}=\hat\phi_{1,(\bar m,\epsilon)}=\begin{pmatrix}\alpha(\epsilon)\exp[-ik_e(\epsilon)z]\\ \exp[-ik_h(\epsilon)z]\end{pmatrix}\psi_{\bar m}(\mathbf{x}_\perp). \tag{A8}$$

The problem now becomes one of computing the mode-space lesser functions $\hat G_{mn}^<(\omega)$. As the only nontrivial interaction in our system is at the impurity itself (the quasiparticles only interact through a hopping term), we may express the exact self-energy appearing in the Dyson equation for $\hat G_{mn}^<(\omega)$ in terms of $\hat D(\omega)$, the Nambu matrix Green function describing the impurity.

The Dyson equation takes the form

$$\begin{aligned}\hat G_{mn}^<=\delta_{mn}\hat G_n^{0,<}+\hat G_m^{0,R}\hat\Sigma_{mn}^<\hat G_n^{0,A}+\hat G_m^{0,R}\hat\Sigma_{mn}^R\hat G_n^{0,<}\\ +\hat G_m^{0,<}\hat\Sigma_{mn}^A\hat G_n^{0,A},\end{aligned} \tag{A9}$$

where the 0 superscript indicates a Green function of the noninteracting system, and the R (A) superscript indicates a retarded (advanced) Green function. All functions in the above formula are to be evaluated at the same frequency. The self-energy matrix appearing in Eq. (A9) is simply

$$[\Sigma_{mn}^R(\omega)]_{ij}=\sum_{\beta,\beta'=1,2}[\hat\phi_{\beta,m}^*(\mathbf{a})]_i D_{\beta\beta'}^R(\omega)[\hat\phi_{\beta',n}(\mathbf{a})]_j \tag{A10}$$

with similar formulas for the advanced and lesser self-energies. Recall that **a** indicates the position of the impurity. This simple form for the self-energy reflects the fact that quasiparticles only interact by hopping on and off the impurity site.

We proceed by substituting Eq. (A9) into Eq. (A3). We evaluate the resulting expression in the limit where z,z' both tend to $-\infty$ (i.e., deep in the normal region). As the wave functions $u_m(\mathbf{x})$ and $v_m(\mathbf{x})$ have a plane wave form, the terms required to calculate the current are greatly simplified. A further simplification arises when we restrict attention only to those quasiparticle modes with energies less than Δ; this is valid for voltages and temperatures which are much smaller than Δ.

After a fair amount of algebra, we obtain a relatively simple formula for the current. Ignoring terms involving the anomalous impurity Green functions for the moment and writing $I=I_0+\delta I$, we have

$$I_0=\frac{2e}{h}\int d\omega \sum_{m,E_m^-<E_F} [f_e(\omega)-f_h(\omega)], \tag{A11}$$

$$\delta I=-\frac{2e}{h}\int d\omega[\pi\Gamma(\omega)]\left(\frac{1}{2\pi i}D_{11}^{<}(\omega)-A_{11}(\omega)f_h(\omega) + \frac{1}{2\pi i}D_{22}^{<}(\omega)-A_{22}(\omega)f_h(\omega)\right). \tag{A12}$$

In the above equations, $f_e(\omega)$ is the distribution function describing electrons, while $f_h(\omega)=1-f_e(-\omega)$ describes holes. $A_{ij}(\omega)=(1/\pi)\mathrm{Im}[D_{ij}^R(\omega)]$ is an impurity spectral function. $\Gamma(\omega)=\pi W^2 N(\omega)$ is an energy-dependent tunneling rate, with $N(\omega)$ being the density of states. Of course, the energy integrals in both these equations should be restricted to values less than Δ due to the approximations that have been made; this will occur naturally for sufficiently small temperatures and voltages.

I_0 in Eq. (A11) is the point contact current in the absence of the impurity. Taking $f_e(\omega)$ to be the shifted Fermi function $f(\omega-eV)$, we find that $G_0=dI_0/dV=(4e^2/h)N_m$, where N_m is the number of transverse modes with energies below the Fermi energy. This is precisely twice the usual Sharvin conductance, and represents the current-doubling effect of Andreev reflection.[20]

Equation (A12) for the modification of the current due to the impurity is still in a somewhat unwieldy form, due to the appearance of the impurity lesser functions. While the *NS*-NCA technique discussed in this paper allows the calculation of spectral functions, it does not allow one to calculate the distribution functions which are necessary to compute the lesser Green function. A similar problem occurs when considering an impurity in a normal point contact,[18] or more generally, the current through an interacting region.[17] In these cases, one can eliminate the lesser function by taking a suitable linear combination of the current computed on the left of the interacting region and that computed on the right. Here, no such simplification is possible, as computing the current within the superconductor is difficult due to the presence of supercurrents.

A means for eliminating the lesser function does however exist. We note that the electron impurity Green functions $D_{11}(\omega)$ are related to the hole impurity Green functions $D_{22}(\omega)$. It follows easily from the definitions of the functions that

$$D_{22}^{<}(\omega)=-D_{11}^{>}(-\omega), \tag{A13}$$

$$A_{22}(\omega)=A_{11}(-\omega), \tag{A14}$$

where the greater Green function $D_{11}^{>}$ is defined by

$$D_{11}^{>}(t)=-i\langle d_\uparrow(t)d_\uparrow^\dagger(0)\rangle. \tag{A15}$$

We use Eqs. (A13) and (A14) to substitute for the third and forth terms in Eq. (A12) for δI. Further, we change the integration variable for these terms from ω to $-\omega$, and make the assumption that $\Gamma(\omega)$ is an even function. The latter is not too severe as long as the temperature and voltage are sufficiently small, as this ensures a small range of ω integration. Finally, we use the relations $f_h(-\omega)=1-f_e(\omega)$ and $D_{11}^{>}-D_{11}^{<}=-2\pi i A_{11}$ to obtain

$$\delta I=-\frac{4e}{h}\int d\omega[\pi\Gamma(\omega)]A_d(\omega)\left(\frac{f_e(\omega)-f_h(\omega)}{2}\right). \tag{A16}$$

Note that A_d in the above formula is the same as A_{11}. Taking Γ to be a constant and differentiating with respect to voltage at V=0 yields the formula (11) for the impurity contribution to the point contact zero-bias conductance.

We now comment on terms in the current which involve anomalous impurity Green functions. Retaining these terms and performing manipulations similar to those described above leads to a second correction term to the point contact current

$$\delta I_{\mathrm{anom}}=-\frac{4e}{h}\int d\omega[\pi\Gamma(\omega)]\left(\frac{\omega}{\Delta}A_{12}(\omega)\right)\left(\frac{f_e(\omega)-f_h(\omega)}{2}\right). \tag{A17}$$

The change to the zero-bias conductance arising from this term is 0 at 0 temperature, and is generally much smaller than δI in Eq. (A16) for temperatures and voltages smaller than Δ. In the case of a strong-U Anderson impurity, $A_{12}(\omega)$ is strongly suppressed due to the suppression of on-site pair correlations. Even in the absence of an on-site repulsion, $A_{12}(\omega)$ is small for $\omega<\Delta$, as there are no nonevanescent quasiparticles in the gap. The presence of the factor ω/Δ further reduces the contribution of this term for small voltages and temperatures. We thus neglect the contribution of this term in computing the point contact zero-bias conductance. Note that we have evaluated numerically the significance of this term in a few test cases by calculating A_{12} within the *NS*-NCA; it typically changes the magnitude of the zero-bias anomaly by less than 0.5%.

[1] A. Golub, Phys. Rev. B **54**, 3640 (1996).

[2] R. Fazio and R. Raimondi, Phys. Rev. Lett. **80**, 2913 (1998); **82**, 4950(E) (1999).

[3] K. Kang, Phys. Rev. B **58**, 9641 (1998).

[4] P. Schwab and R. Raimondi, Phys. Rev. B **59**, 1637 (1999).

[5] D. Goldhaber-Gordon, J. Göres, M. A. Kastner, H. Shtrikman, D. Mahalu, and U. Meirav, Phys. Rev. Lett. **81**, 5225 (1998).

[6] S. M. Cronenwett, T. H. Oosterkamp, and L. P. Kouwenhoven, Science **281**, 540 (1998).

[7] D. C. Ralph, A. W. W. Ludwig, J. von Delft, and R. A. Buhrman, Phys. Rev. Lett. **72**, 1064 (1994); D. C. Ralph and R. A. Buhrman, *ibid.* **72**, 3401 (1994).

[8] S. K. Upadhyay, R. N. Louie, and R. A. Buhrman, Phys. Rev. B **56**, 12 033 (1997).

[9] S. K. Upadhyay, A. Palanisami, R. N. Louie, and R. A. Buhrman, Phys. Rev. Lett. **81**, 3247 (1998).

[10] See, e.g., J. von Delft, D. C. Ralph, R. A. Buhrman, S. K. Upadhyay, R. N. Louie, A. W. W. Ludwig, and V. Ambegaokar, Ann. Phys. (N.Y.) **263**, 1 (1998).

[11] N. E. Bickers, Rev. Mod. Phys. **59**, 845 (1987), and references cited within.

[12] Though $1/N=1/2$ is not a small parameter in the present context, large-N approaches can still retain validity. As discussed in Ref. 11, they provide a systematic means of organizing perturbation theory in a manner which captures the essence of Kondo physics (i.e., the formation of a singlet ground state in the one-channel case). This does not occur if one attempts a perturbative expansion in the hopping parameter W.

[13] Y. Kuramoto, Z. Phys. B: Condens. Matter **53**, 37 (1983).

[14] O. Gunnarsson and K. Schonhammer, Phys. Rev. B **31**, 4815 (1985).

[15] In the clean limit, the usual gapped density of states is only recovered when one moves a coherence length into the superconductor, at which point the contribution from evanescent quasiparticle modes is negligible.

[16] Recall that for an Anderson impurity, T_K is proportional to exp $(-\pi|\varepsilon_d|/2\Gamma)$.

[17] Y. Meir and N.S. Wingreen, Phys. Rev. Lett. **68**, 2512 (1992).

[18] M. H. Hettler, J. Kroha, and S. Hershfield, Phys. Rev. B **58**, 5649 (1998).

[19] N. E. Bickers and G. E. Zwicknagl, Phys. Rev. B **36**, 6746 (1987).

[20] C. W. J. Beenakker, Rev. Mod. Phys. **69**, 731 (1997).